

# Application of NiMoO<sub>4</sub> Nanorods for the Direct Electrochemistry and Electrocatalysis of Hemoglobin with Carbon Ionic Liquid Electrode

Song Hu,<sup>a</sup> Lili Cao,<sup>b</sup> Zhaolan Sun,<sup>b</sup> Jun Xiang,<sup>a</sup> Ming Lu,<sup>b</sup> Wei Sun<sup>\*b</sup>

<sup>a</sup> State Key Laboratory of Coal Combustion, Huazhong University of Science and Technology, Wuhan 430074, P. R. China

<sup>b</sup> Shandong Provincial Key Laboratory of Biochemical Analysis, College of Chemistry and Molecular Engineering, Qingdao University of Science and Technology, Qingdao 266042, P. R. China

\*e-mail: sunwei@qust.edu.cn

Received: September 12, 2011

Accepted: November 27, 2011

## Abstract

In this paper NiMoO<sub>4</sub> nanorods were synthesized and used to accelerate the direct electron transfer of hemoglobin (Hb). By using an ionic liquid (IL) 1-butylpyridinium hexafluorophosphate (BPPF<sub>6</sub>) modified carbon paste electrode (CILE) as the basic electrode, NiMoO<sub>4</sub> nanorods and Hb composite biomaterial was further cast on the surface of CILE and fixed by chitosan (CTS) to establish a modified electrode denoted as CTS/NiMoO<sub>4</sub>-Hb/CILE. UV-vis and FT-IR spectroscopic results showed that Hb in the film retained its native structures without any conformational changes. Electrochemical behaviors of Hb entrapped in the film were carefully investigated by cyclic voltammetry with a pair of well-defined and quasi-reversible redox voltammetric peaks appearing in phosphate buffer solution (PBS, pH 3.0), which was attributed to the direct electrochemistry of the electroactive center of Hb heme Fe(III)/Fe(II). The results were ascribed to the specific characteristic of NiMoO<sub>4</sub> nanorods, which accelerated the direct electron transfer rate of Hb with the underlying CILE. The electrochemical parameters of Hb in the composite film were further carefully calculated with the results of the electron transfer number ( $n$ ) as 1.08, the charge transfer coefficient ( $\alpha$ ) as 0.39 and the electron-transfer rate constant ( $k_s$ ) as 0.82 s<sup>-1</sup>. The Hb modified electrode showed good electrocatalytic ability toward the reduction of trichloroacetic acid (TCA) in the concentration range from 0.2 to 26.0 mmol/L with a detection limit of 0.072 mmol/L (3 $\sigma$ ), and H<sub>2</sub>O<sub>2</sub> in the concentration range from 0.1 to 426.0  $\mu$ mol/L with a detection limit of 3.16  $\times 10^{-8}$  mol/L (3 $\sigma$ ).

**Keywords:** Hemoglobin, NiMoO<sub>4</sub> nanorods, Ionic liquid, Carbon paste electrode, Electrochemistry

DOI: 10.1002/elan.201100508

## 1 Introduction

Direct electron transfer of enzymes or proteins with working electrode is one of the enduring challenges in the electrochemical field. The study on the direct electron transfer can offer an electrochemical basis for the investigation on the structure of redox enzymes, the redox mechanisms of enzymes, and metabolic process involving redox transformations. Also the results can be used to establish different types of biosensors, catalytic bioreactors and biomedical devices [1]. However, it is difficult to realize the direct electron transfer between redox proteins and electrodes directly due to the reasons such as the three-dimensional structure of proteins hindered the interaction of the electroactive centers with the electrode, the denaturation and unfavorable orientations of proteins upon adsorption onto the surface of the electrode, and subsequent passivation of the electrode surface [2]. Extensive researches have been done over the last twenty years to solve these problems and accelerate the direct electron transfer of redox proteins. Different kinds of films modified electrodes such as insoluble surfactants

[3], hydrogels [4,5], biopolymers [6,7], composite films [8,9], nanoparticles [10] and polyions grown layer-by-layer [11,12] have been devised for the electrochemical behaviors of redox proteins and further applied to biosensors and biocatalysis, which could facilitate faster direct electron transfer between the proteins and the electrode.

Recently different kinds of nanoparticles had been applied to protein electrochemistry due to their unique properties such as large surface area, high thermal and chemical stability, tunable porosity, biocompatibility and catalytic activities [13]. Nanoparticles can be used not only for the preparation of modified electrodes but also acceleration of the electron transfer rate. Different kinds of nanoparticles, including carbon nanotube (CNT), metal nanoparticles, semi-conductor nanoparticles, had been used in the protein electrochemistry. For example, Hu et al. applied different nanoparticles such as SiO<sub>2</sub> [14], Fe<sub>3</sub>O<sub>4</sub> [15], Au [16], and CNT [17] in the layer-by-layer self-assembly with heme protein to establish electrochemical biosensor. Wang et al. [18] investigated the direct electrochemistry and electrocatalysis of hemoglobin (Hb) adsorbed in gold nanoshells. Xue et al. [19] also

studied the direct electrochemistry of Hb entrapped in a composite film based on chitosan and  $\text{CaCO}_3$  nanoparticles.  $\text{NiMoO}_4$  nanoparticles are semiconductors with the advantages of high surface area, optical transparency, good biocompatibility, relatively good conductivity and are of great importance in heterogeneous catalysis and in industrial application. But there are few reports with the application of  $\text{NiMoO}_4$  nanoparticles for the protein electrochemistry.

In recent years, ionic liquids (ILs) had been widely used in the fields of electrochemistry and electroanalysis due to the advantages such as high chemical and thermal stability, relatively high ionic conductivity, negligible vapor pressure and wider electrochemical windows [20–22]. By using IL in the traditional carbon paste electrode as binder and modifier, carbon ionic liquid electrode (CILE) has been proven to exhibit excellent electrochemical performances than traditional glassy carbon electrode (GCE) or carbon paste electrode (CPE). So CILE has been used as the working electrode in the field of electrochemical sensors with the advantages such as resistivity towards electrode fouling, high rates of electron transfer and the inherent catalytic activity. Maleki et al. [23] applied *N*-octylpyridinium hexafluorophosphate (OPFP) as a binder for the construction of CILE and investigated the electrochemical behaviors of some electroactive compounds. Sun [24] applied *N*-butylpyridinium hexafluorophosphate (BPPF<sub>6</sub>) based CILE for the electrochemical detection of hemoglobin. Also different kinds of modifiers were cast on the CILE surface and used for the protein electrochemistry [25–27].

In this paper a CILE was prepared and used as the substrate electrode for the electrochemical measurement. Then the  $\text{NiMoO}_4$  nanorod and Hb composite was modified on the surface of CILE. By using chitosan (CTS) as the film forming material, the modifiers were fixed on the CILE surface tightly. CTS has been widely reported as an immobilization matrix for the preparation of biosensor and bioreactor [28–31], which exhibits excellent film-forming ability as a biocompatible, biodegradable and nontoxic natural biopolymer. Then the Hb modified electrode (CTS/ $\text{NiMoO}_4$ -Hb/CILE) was constructed and its electrochemical behaviors were investigated carefully. Due to the specific properties of  $\text{NiMoO}_4$  nanorods such as good biocompatibility, large surface area, good dispersing properties and fast electron transfer ability, the direct electron transfer of Hb with the underlying CILE was achieved on the modified electrode. Spectroscopic results indicated that Hb in the film retained its native structure. The modified electrode exhibited good electrocatalytic activity to the reduction of trichloroacetic acid (TCA) and hydrogen peroxide ( $\text{H}_2\text{O}_2$ ).

## 2 Experimental

### 2.1 Reagents

Bovine hemoglobin (Hb, MW. 64500, Tianjin Chuanye Biochemical Limited Company), ionic liquid 1-butylpyridinium hexafluorophosphate (BPPF<sub>6</sub>, Lanzhou Greenchem ILS, LICP. CAS. China), chitosan (CTS, minimum 95% deacetylated, Dalian Xindie Chemical Reagents Limited Company), graphite powder (average particle size 30  $\mu\text{m}$ , Shanghai Colloid Chemical Plant) and trichloroacetic acid (TCA, Tianjin Kemiou Chemical Limited Company) were used as received.  $\text{NiMoO}_4$  nanorods (nano- $\text{NiMoO}_4$ ) were synthesized according to the reference [32]. 0.1 mol/L phosphate buffer solutions (PBS) with various pH values were prepared by mixing stock standard solutions of  $\text{K}_2\text{HPO}_4$  with  $\text{KH}_2\text{PO}_4$  and used as the supporting electrolyte. All the other chemicals were of analytical reagent grade and doubly distilled water was used in all the experiments.

### 2.2 Apparatus

A CHI 750B electrochemical workstation (Shanghai CH Instrument, China) was used for electrochemical measurements with a conventional three-electrode system composed of a modified CILE as working electrode, a saturated calomel electrode (SCE) as reference electrode and a platinum wire as counter electrode. All the potentials were given with respect to SCE. UV–visible absorption spectrum was operated with a Cary 50 probe spectrophotometer (Varian Company, Australia). Fourier-transform infrared (FT-IR) spectrum was obtained on a Tensor 27 FT-IR spectrophotometer (Bruker, Germany). Scanning electron microscopy (SEM) was conducted with a JSM-6700F scanning electron microscope (Japan Electron Company).

### 2.3 Electrode Preparation

Ionic liquid modified carbon paste was fabricated by mixing 0.5 g of BPPF<sub>6</sub> and 1.5 g of graphite powder in a mortar. After grinding carefully, a portion of the homogeneous paste was packed into a glass tube ( $\varnothing = 4.2$  mm) and the electrical contact was established through a copper wire at the end of the paste in the inner hole of the tube. Then the surface of CILE was polished on a weighing paper just before use.

A mixture solution containing 12.0 mg/mL Hb and 0.5 mg/mL nano- $\text{NiMoO}_4$  was prepared and mixed homogeneously to obtain a suspension solution. Then 10  $\mu\text{L}$  of the mixture solution was evenly dropped onto the surface of the CILE, spread gently over the entire surface, and then the electrode was left in the air to allow the water evaporate gradually. Finally, 5.0  $\mu\text{L}$  of a 1.0 mg/mL CTS (in 1.0% HAC) solution was applied on the electrode surface and dried to get a uniform film modified electrode. The fabricated electrode was denoted as CTS/ $\text{NiMoO}_4$ -

Hb/CILE and kept at 4 °C refrigerator when not use. For comparison other modified electrodes such as CTS/CILE, CTS/Hb/CILE etc. were prepared with similar procedures.

## 2.4 Electrochemical Measurements

Electrochemical measurements were performed at room temperature ( $20 \pm 2$  °C) by using a CHI 750B electrochemical workstation with cyclic voltammetry. The working buffer solutions were deoxygenated by bubbling high pure nitrogen thoroughly for at least 30 min before the experiments and the nitrogen atmosphere environment was kept in the electrochemical cell during the procedure. The three-electrode system was immersed in a 10 mL cell containing 0.1 mol/L pH 3.0 PBS and scanned in the potential range from 0.2 to  $-0.6$  V (vs. SCE) at the scan rate of 100 mV/s. Electrochemical impedance spectroscopy (EIS) was performed in a 10.0 mmol/L  $[\text{Fe}(\text{CN})_6]^{3-/4-}$  solution with the frequencies swept from  $10^5$  to  $10^{-1}$  Hz.

## 3 Results and Discussion

### 3.1 SEM images of NiMoO<sub>4</sub> Nanorods

Scanning electron microscopy (SEM) was used to record the morphologies of NiMoO<sub>4</sub> nanorods. The results are shown in Figure 1. The SEM image indicated that NiMoO<sub>4</sub> nanomaterials were composed entirely of rod like nanostructures with a width of about 200 nm and a length of several micrometers. As obvious from the images, some of the nanorods were aggregated to form bundles and the inset was SEM image of NiMoO<sub>4</sub> nanorods with large magnification.

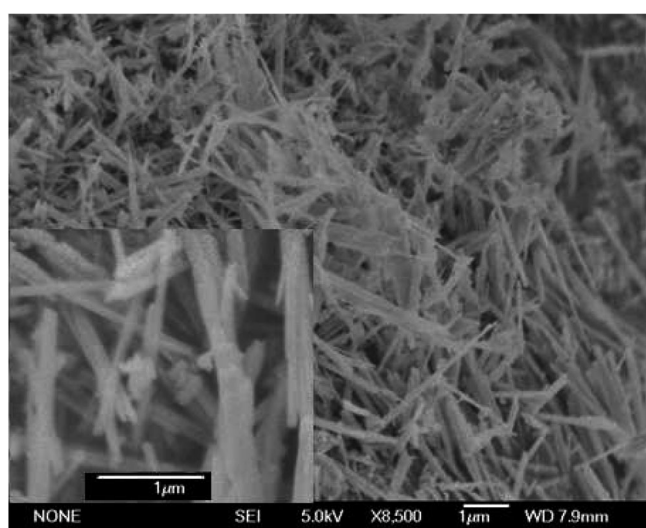


Fig. 1. SEM images of NiMoO<sub>4</sub> nanorods. Inset: High magnification SEM image.

### 3.2 FT-IR and UV-Vis Absorption Spectroscopy

The secondary structure of the heme proteins can be further confirmed with FT-IR spectroscopy. It is well-known, that the position of amide I ( $1700\text{--}1600$   $\text{cm}^{-1}$ ) and amide II ( $1620\text{--}1500$   $\text{cm}^{-1}$ ) can provide detailed information on the secondary structure of the polypeptide chain. As can be seen from Figure 2A, the amide I and amide II bands of native Hb are located at  $1653$  and  $1536$   $\text{cm}^{-1}$  (curve a). After mixing CTS, NiMoO<sub>4</sub> and Hb together, the FTIR spectrum has similar shapes to that of native Hb, with the amide I and amide II bands only shifted slightly to  $1651$  and  $1532$   $\text{cm}^{-1}$  (curve b), respectively. The results proved that the secondary structure of Hb molecules kept almost unchanged after immobilized within CTS and NiMoO<sub>4</sub> composite film.

UV-vis spectroscopy is another effective tool for monitoring the possible change of the Soret absorption band in the heme group. The band shift may provide conformational information about the denaturation on the tertiary structure of heme proteins [33]. Figure 2B displayed the UV-vis spectra of Hb in the composite material. It can be seen that the native Hb gave a Soret absorption band at 406 nm in pH 3.0 PBS (curve a). While in the CTS/NiMoO<sub>4</sub>-Hb composite film the Soret band also appeared at 406 nm without changes (curve b), suggesting that the native structure of Hb was not changed after immobilized in the CTS and NiMoO<sub>4</sub> composite film. So the composite film provided a suitable microenvironment to keep the native structure of Hb, which can be attributed to the good biocompatibility of CTS and nano-NiMoO<sub>4</sub> used. NiMoO<sub>4</sub> nanorods are biocompatible nanomaterials with high surface area, which can provide a specific interface for Hb immobilization.

### 3.3 Electrochemical Impedance Spectroscopy

Electrochemical impedance spectroscopy (EIS) can provide the impedance changes during the electrode modification process. The diameter of the semicircle usually equals to the electron transfer resistance ( $R_{\text{et}}$ ), which controls the electron transfer kinetics of the redox probe at the electrode interface. EIS experiments were performed in 0.1 mol/L KCl solution containing 10.0 mmol/L  $[\text{Fe}(\text{CN})_6]^{3-/4-}$  with the frequencies swept from  $10^5$  to  $10^{-1}$  Hz. Figure 3 showed the EIS results of CTS/NiMoO<sub>4</sub>-Hb/CILE (curve a), bare CILE (curve b), CTS/CILE (curve c), CTS/Hb/CILE (curve d), respectively. The  $R_{\text{et}}$  value of CILE was got as  $44.37$   $\Omega$ , which was due to the presence of high conductive ILs in the carbon paste. When a CTS layer was immobilized on the surface of CILE, the  $R_{\text{et}}$  value increased to  $52.44$   $\Omega$ , indicating that the presence of nonconductive CTS film on the electrode surface decreased the electron transfer rate. On the CTS/Hb/CILE the  $R_{\text{et}}$  value further increased to  $150.5$   $\Omega$ , which indicated that the presence of Hb molecules in the film on the electrode surface further hindered the electron transfer rate of  $[\text{Fe}(\text{CN})_6]^{3-/4-}$ . While on the CTS/

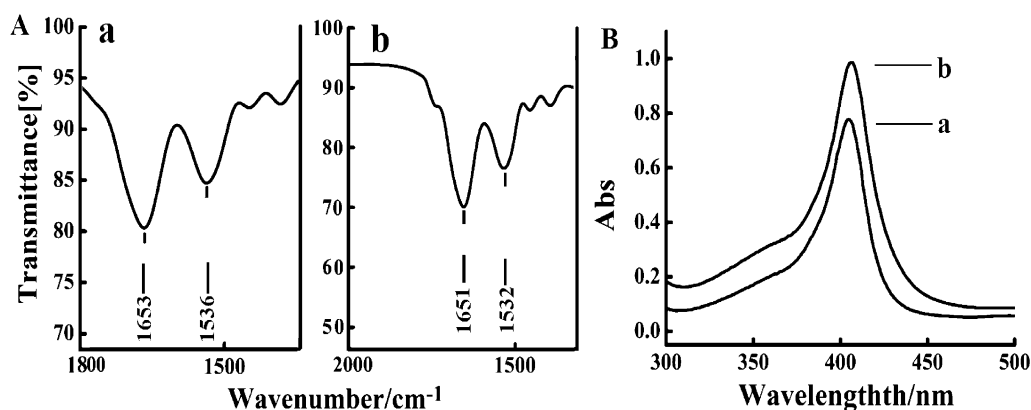


Fig. 2. (A) FT-IR spectra of (a) Hb film; (b) CTS/NiMoO<sub>4</sub>-Hb composite film; (B) UV-vis absorption spectra of native Hb and CTS/NiMoO<sub>4</sub>-Hb composite film in pH 3.0 PBS, respectively.

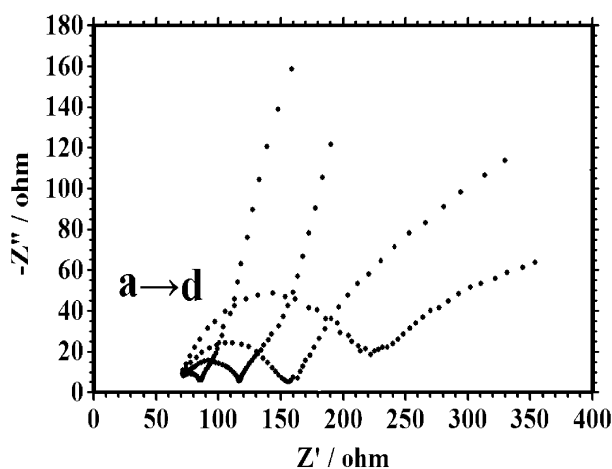


Fig. 3. Electrochemical impedance spectroscopy of (a) CTS/NiMoO<sub>4</sub>-Hb/CILE, (b) bare CILE, (c) CTS/CILE and (d) CTS/Hb/CILE in the presence of 10.0 mmol/L [Fe(CN<sub>6</sub>)]<sup>3-/4-</sup> + 0.1 mol/L KCl with the frequencies swept from 10<sup>5</sup> to 10<sup>-1</sup> Hz.

NiMoO<sub>4</sub>-Hb/CILE, the  $R_{et}$  value decreased to 13.25  $\Omega$ , indicating that the addition of good conductive NiMoO<sub>4</sub> nanorods in the film increased the electron transfer rate and decreased the resistance of the electrode surface. NiMoO<sub>4</sub> nanorods are semiconductors with the advantages of high surface area, optical transparency, good biocompatibility, and relatively good conductivity, which exhibited good electrochemical behaviors on the electrode surface.

### 3.4 Optimization of the Electrode Preparation

The optimal ratio of graphite powder and BPPF<sub>6</sub> for the preparation of CILE was investigated with different weight ratio such as 5:1, 4:1, 3:1 and 2:1 (w/w), respectively. By comparing the electrochemical response of CILEs in the ferricyanide solution, a final 3:1 (w/w) ratio was selected as the optimized composition, which gave the highest redox peaks and the smallest peak-to-peak separation.

Also the composition of the modifier on the electrode surface was optimized to get the most stable and highest cyclic voltammetric responses of Hb. By varying the ratio of Hb, NiMoO<sub>4</sub> nanorods and CTS in the nanocomposite, direct electrochemistry of the Hb modified electrode was investigated in the control experiments. Experimental results showed that the amount of NiMoO<sub>4</sub> and CTS nanorods had great influences on the electrochemical responses of the modified electrode. The presence of NiMoO<sub>4</sub> nanorods can provide a specific interface with high surface area, but excessive amount of NiMoO<sub>4</sub> nanorods on the electrode surface will increase the thickness of the film and finally result in the cracking of the composite film. Also CTS exhibited good film forming ability for the stability of the modified electrode. The composite without the CTS was not stable and the modifier could be easily leaked out to the buffer solution. At last the composite film that containing 12.0 mg/mL Hb, 0.5 mg/mL nano-NiMoO<sub>4</sub> and 1.0 mg/mL CTS was selected as the optimal ratio for the fabrication of modified electrode.

### 3.5 Direct Electrochemistry of the Hb Modified Electrode

Figure 4 showed cyclic voltammograms of different modified electrodes in pH 3.0 PBS at the scan rate of 100 mV/s. No electrochemical responses were observed at CILE (curve a) and CTS/CILE (curve b), which indicated no electroactive substances existed on the surface of electrode. On CTS/Hb/CILE (curve c) a pair of redox peaks appeared, which revealed that direct electron transfer between Hb and CILE was achieved with slow electron transfer rate. The result was similar to the former report [34], which was attributed to the specific characteristics of CILE such as high conductivity with a layer of IL film present on the electrode surface. So the electron transfer of Hb with CILE was realized. After the addition of NiMoO<sub>4</sub> nanorod in the film, a pair of well-defined and quasi-reversible redox peaks appeared with the increase of electrochemical responses (curve d). The redox peak current was 2.25 times higher than that of CTS/Hb/CILE

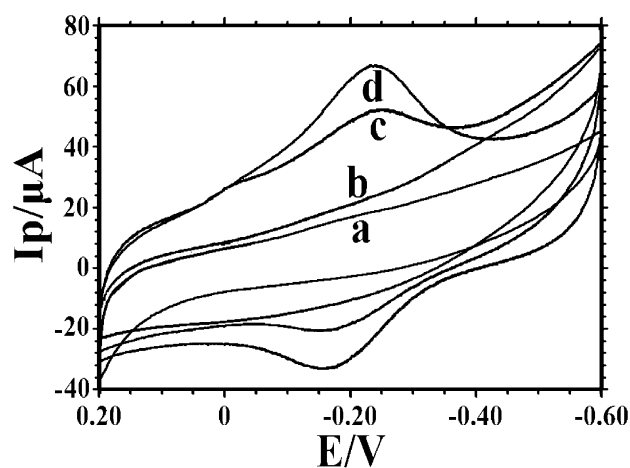


Fig. 4. Cyclic voltammograms of (a) CILE, (b) CTS/CILE, (c) CTS/Hb/CILE and (d) CTS/NiMoO<sub>4</sub>-Hb/CILE in pH 3.0 PBS at the scan rate of 100 mV/s.

at the scan rate of 100 mV/s, which was attributed to the presence of NiMoO<sub>4</sub> nanorods with good conductivity and biocompatibility incorporated in the film. The oxidation potential ( $E_{pa}$ ) and the reduction potential ( $E_{pc}$ ) were located at  $-0.152$  V and  $-0.231$  V, respectively. The formal potential ( $E^{\circ}$ ) was estimated to be  $-0.192$  V (vs. SCE) and the peak-to-peak potential separation ( $\Delta E_p$ ) was 79 mV with equal high of the redox peak current. The result means that Hb undergone a quasi-reversible electrochemical reaction. Due to the co-contribution of CTS and nano-NiMoO<sub>4</sub> present on the surface of CILE, the direct electrochemistry of Hb, which was derived from the heme Fe(III)/Fe(II) redox couples, was achieved.

It is well-known that most of the heme proteins exhibit a pH-dependent conformational equilibrium and the pH value of the buffer solution influences the electrochemical reaction of the heme proteins. The effect of pH of the buffer solution on the response of the CTS/NiMoO<sub>4</sub>-Hb/CILE was investigated in the pH range from 1.0 to 7.0. The increase of buffer pH led to a negative shift of both reduction and oxidation peak potentials, which indicated that protons involved in the electrode reaction. The maximum redox peak currents were got at pH 3.0 buffer solution, which was selected for the further investigation.

### 3.6 Effect of Scan Rate

The effect of scan rate on the cyclic voltammetric response of the immobilized Hb was investigated and the results were shown in Figure 5. With the increase of scan rate from 50 to 500 mV/s, the cathodic and anodic peak currents of Hb increased gradually with approximately equal height. Two linear regression equations were calculated as  $I_{pc}$  ( $\mu\text{A}$ ) =  $160.5 v$  (V/s) +  $4.478$  ( $\gamma = 0.996$ ) and  $I_{pa}$  ( $\mu\text{A}$ ) =  $-161.7 v$  (V/s) -  $12.47$  ( $\gamma = 0.995$ ), respectively. This indicated that the electron transfer process of CTS/NiMoO<sub>4</sub>-Hb/CILE was a typical surface-confined electro-

chemical behavior in above-mentioned potential scope. The surface concentration ( $\Gamma^*$ ) of the electroactive Hb can be further estimated by integration of the cyclic voltammetric reduction peaks based on the formula  $Q = nFA\Gamma^*$  [35], where  $Q$  is the integration charge of the reduction peak,  $n$  is the number of electrons transferred,  $F$  is the Faraday constant,  $A$  is the geometric area of the modified electrode. The charge value ( $Q$ ) was nearly constant at different scan rates and the average value of  $\Gamma^*$  was calculated as  $1.87 \times 10^{-9}$  mol/cm<sup>2</sup>, which was much larger than that of monolayer coverage ( $1.89 \times 10^{-11}$  mol/cm<sup>2</sup>). While the total surface concentration of Hb in the composite film cast on the electrode was calculated as  $1.48 \times 10^{-8}$  mol/cm<sup>2</sup>, so 12.64% of the immobilized Hb took part in the electrode reaction. The results demonstrated that the composite film is efficiency for Hb immobilization and the presence of NiMoO<sub>4</sub> nanorods on CILE gave a much higher surface area to immobilize Hb and the interaction of NiMoO<sub>4</sub> nanorods with Hb happened in the film, which resulted in the several layers of Hb immobilized near the electrode surface underwent the electrochemical reaction.

With the increase of scan rate the redox peak potential shifted slightly with the peak-to-peak separation increased gradually. The redox peak potentials ( $E_p$ ) were linearly dependent on the natural logarithm of scan rate ( $v$ ) with the equations as  $E_{pc}$  (V) =  $-0.0612 \ln v - 0.288$  ( $\gamma = 0.9988$ ) and  $E_{pa}$  (V) =  $0.0387 \ln v - 0.122$  ( $\gamma = 0.9984$ ) respectively. The electrochemical parameters of Hb in the composite film were calculated according to the following Laviron's equation: [36,37]

$$E_{pc} = E^{\circ} - \frac{RT}{\alpha nF} \ln v \quad (1)$$

$$E_{pa} = E^{\circ} + \frac{RT}{(1-\alpha)nF} \ln v \quad (2)$$

$$\log k_s = \alpha \log(1-\alpha) + (1-\alpha) \log \alpha - \log \frac{RT}{nFv} - \frac{(1-\alpha)\alpha nF \Delta E_p}{2.3RT} \quad (3)$$

where  $\alpha$  is the electron transfer coefficient,  $n$  is the number of electron transferred,  $v$  is the scan rate, and  $E^{\circ}$  is the formal potential,  $k_s$  is the electron transfer rate constant and  $\Delta E_p$  is the peak to peak potential separation.  $R$ ,  $T$  and  $F$  have their conventional meanings. The value of  $n$  was estimated as 1.08, suggesting that nearly one electron was involved in the reaction. The values of  $\alpha$  and  $k_s$  can be easily calculated as 0.39 and  $0.82 \text{ s}^{-1}$ . The value of  $k_s$  is bigger than some previous reported values of  $0.34 \text{ s}^{-1}$  on Mb/NiO/GCE [38] and 0.41 on Mb-HSG-SN-CNTs/GCE [39], indicating that NiMoO<sub>4</sub> nanorod was an excellent promoter for the direct electron transfer.

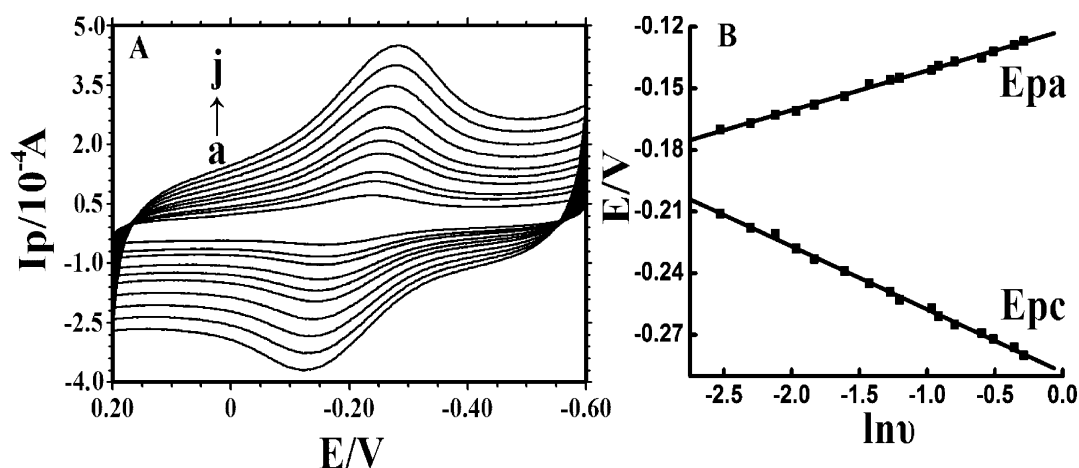


Fig. 5. (A) Cyclic voltammograms of CTS/NiMoO<sub>4</sub>-Hb/CILE in pH 3.0 PBS with different scan rates (a–j: 80, 100, 160, 200, 280, 340, 400, 500, 600, 700 mV/s); (B) The relationship of the anodic and cathodic peak potential against  $\ln v$ .

### 3.7 Electrocatalytic Properties of CTS/NiMoO<sub>4</sub>-Hb/CILE

The redox proteins usually have good electrocatalytic activity towards different substrates such as trichloroacetic acid (TCA) and H<sub>2</sub>O<sub>2</sub>, so the electrocatalytic activity of CTS/NiMoO<sub>4</sub>-Hb/CILE was investigated. Figure 6 showed the electrocatalytic reduction of TCA on CTS/NiMoO<sub>4</sub>-Hb/CILE by cyclic voltammetry. With the addition of different amounts of TCA into PBS, a significant increase of the reduction peak current was observed at -0.231 V (vs.SCE) accompanying with the disappearance of the oxidation peak current, demonstrating a typical electrocatalytic reduction process of TCA. The catalytic peak current increased with the TCA concentration in the range from 0.2 to 26.0 mmol/L with the linear regression equation as  $I_{ss}$  ( $\mu A$ ) = 3.467C (mmol/L) + 28.50 ( $n = 17$ ,  $\gamma = 0.998$ ) and the detection limit as 0.072 mmol/L ( $3\sigma$ ), which was lower than that of the previous results of 0.1 mmol/L on Nafion/Mb/MWCNTs/CILE [25],

0.13 mmol/L on Nafion/Hb/DNA/CILE [40] and 0.16 mmol/L on Nafion/Hb/Au/CILE [41].

When the TCA concentration was more than 26.0 mmol/L the catalytic reduction peak currents began to level off and reached a response plateau, indicating a Michaelis–Menten kinetic mechanism. The apparent Michaelis–Menten constant ( $K_M^{app}$ ), which gave an indication of the enzyme–substrate kinetics, could be calculated from the electrochemical version of the Lineweaver–Burk equation [42]:

$$\frac{1}{I_{ss}} = \frac{1}{I_{max}} + \frac{K_M^{app}}{I_{max}c} \quad (4)$$

where  $I_{ss}$  is the steady current after the addition of substrate,  $c$  is the bulk concentration of the substrate, and  $I_{max}$  is the maximum current measured under saturated substrate condition. Based on the above equation the  $K_M^{app}$  value was calculated as 0.735 mmol/L, which is smaller than the reported values of 14.52 mmol/L on

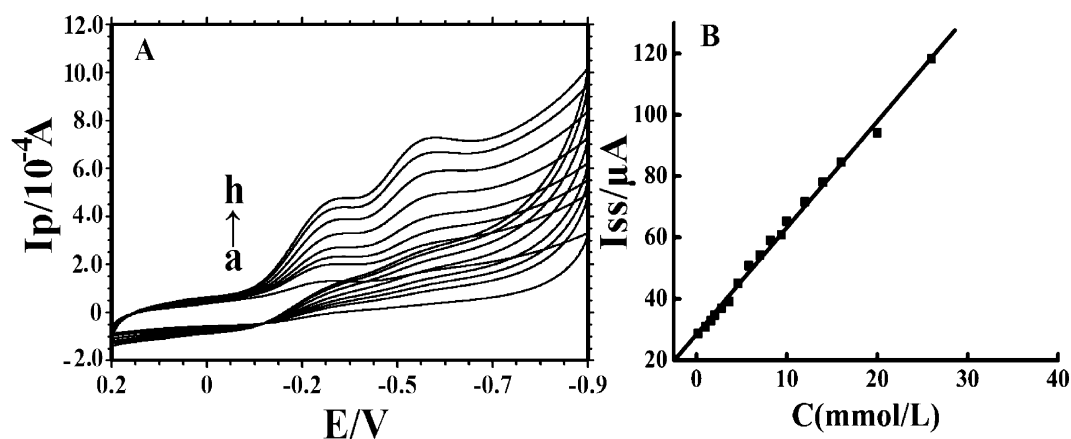


Fig. 6. (A) Cyclic voltammograms of CTS/NiMoO<sub>4</sub>-Hb/CILE in the presence of 2.0, 4.0, 5.2, 6.4, 8.2, 12.0, 16.0, 22.0 mol/L TCA (a–h) in pH 3.0 PBS at the scan rate of 100 mV/s; (B) Linear relationship of catalytic reduction peak currents and the TCA concentration.

Table 1. Detection results of H<sub>2</sub>O<sub>2</sub> in disinfectant sample ( $n=3$ ).

Sample	Detected (mM)	Added (mM)	Found (mM)	Recovery (%)	RSD (%)
1	0.162	0.100	0.266	104.0	1.27
2	0.158	0.150	0.312	102.7	1.39
3	0.153	0.200	0.345	96.0	2.51

Nafion/Hb-CNT/CPE [43] and 47 mmol/L on Hb-agarose/GCE [44], which indicated that the Hb immobilized on the electrode surface exhibited a high affinity to TCA reduction.

The electrocatalytic activity of the CTS/NiMoO<sub>4</sub>-Hb/CILE towards H<sub>2</sub>O<sub>2</sub> was also investigated. When different amounts of H<sub>2</sub>O<sub>2</sub> solution were added to PBS, a significant increase of reduction peak current were observed at -0.24 V with the decrease of the oxidation peak current, indicating the electrocatalytic reduction to H<sub>2</sub>O<sub>2</sub>. Furthermore, the reduction peak current increased linearly with H<sub>2</sub>O<sub>2</sub> concentration in the range from 0.1 to 426.0 μmol/L with the linear regression equation as  $I_{ss} (\mu A) = 0.076 C (\mu mol/L) + 10.76$  ( $n=18$ ,  $\gamma=0.9958$ ) and the detection limit as  $3.16 \times 10^{-8}$  mol/L ( $3\sigma$ ), which was smaller than some previous reported values of  $3.6 \times 10^{-7}$  mol/L on Mb-HSG-SN-CNTs/GCE [39],  $4 \times 10^{-7}$  mol/L on DNA-Hb modified gold electrode [45] and  $1.0 \times 10^{-6}$  mol/L on Hb/CILE [46]. The apparent Michaelis-Menten constant ( $K_M^{app}$ ) was further calculated as 0.0894 mmol/L, which was lower than the reported values of 0.136 mmol/L on Hb-Nafion-Co<sub>3</sub>O<sub>4</sub>/GCE [47] and 1.4 mmol/L on Hb/Chit-Aus/Cys/Au electrode [48]. The results indicated an obvious stronger interaction of Hb with H<sub>2</sub>O<sub>2</sub>.

Different kinds of possible interfering substances were used to evaluate the selectivity of the biosensor. For the determination of  $2.0 \times 10^{-5}$  mol/L H<sub>2</sub>O<sub>2</sub>, no significant interferences could be observed for substances such as Al<sup>3+</sup>, Mn<sup>2+</sup>, Co<sup>2+</sup>, Ni<sup>2+</sup>, Sn<sup>2+</sup>, L-arginine, L-tryptophan, L-cysteine, L-valine, L-leucine, glycine, guanosine, thymine, RNA, DNA etc. at the concentration of 30 fold higher than that of H<sub>2</sub>O<sub>2</sub> in the selected potential range. So the proposed bioelectrode showed good selectivity for the H<sub>2</sub>O<sub>2</sub> detection.

### 3.8 Analytical Application

To test the analytical application of this electrochemical method, the fabricated electrode was applied to detect the H<sub>2</sub>O<sub>2</sub> concentration in the disinfectant samples, which was produced by Xintai Hongshui Pharmaceutical Co., Ltd with the specified amount as 26.35 mg/mL. The sample was firstly diluted for 5,000 times with double distilled water and further detected by the experimental procedure. Under the optimal conditions with the standard addition method, the determination results were summarized in Table 1. It can be seen that the samples were satisfactory detected with the recoveries in the range of 96.0–104.0%, indicating the potential applications in the real samples.

### 3.8 Stability and Reproducibility

The stability of the CTS/NiMoO<sub>4</sub>-Hb/CILE was further studied by electrochemical method. After the Hb modified electrode was stored in a refrigerator at 4°C for two weeks, the 2.84% decrease of redox peak current appeared. After a 30-day storage period, the CTS/NiMoO<sub>4</sub>-Hb/CILE still retained 92.6% of its initial current response, which indicated that the Hb electrode had good stability. Furthermore, the reproducibility of the modified electrode was investigated. Four modified electrodes fabricated with the same procedure were used for the detection of 20.0 mmol/L TCA, which gave an acceptable reproducibility with a relative standard deviation (RSD) of 3.25%. Thus, the CTS/NiMoO<sub>4</sub>-Hb/CILE exhibited good stability and reproducibility for the electrochemical detection in general.

## 4 Conclusions

In this paper NiMoO<sub>4</sub> nanorods were used as an efficient promoter for the acceleration of the direct electron transfer of Hb. Based on CTS and nano-NiMoO<sub>4</sub>, a novel composite material was fabricated and used as an immobilization matrix to fix Hb molecules on the electrode surface. Direct electrochemistry of Hb was achieved on the modified electrode with a pair of well-defined quasi-reversible redox peaks appeared, which was due to the presence of NiMoO<sub>4</sub> nanorods on the electrode surface that accelerated the electron transfer rate. The resulting electrode exhibited a good electrocatalytic activity towards TCA and H<sub>2</sub>O<sub>2</sub> with a wider linearity range and a lower detection limit. So the NiMoO<sub>4</sub> nanorods can be served for the fabrication of the third generation electrochemical biosensors with the advantages such as good stability, high electrocatalytic ability, and simply preparation procedure.

## Acknowledgements

We are grateful to the financial support of the Natural Science Foundation of China (No. 50976043), the Foundation of the State Key Laboratory of Coal Combustion of Huazhong University of Science and Technology (FSKLCC1010) and the Foundation of the State Key Laboratory of Clean Energy Utilization of Zhejiang University.

## References

- [1] S. Zhao, K. Zhang, Y. Bai, W. W. Yang, C. Q. Sun, *Bioelectrochemistry* **2006**, *69*, 158.
- [2] G. C. Zhao, L. Zhang, X. W. Wei, *Anal. Biochem.* **2004**, *329*, 160.
- [3] A. E. F. Nassar, Z. Zhang, N. F. Hu, J. F. Rusling, T. F. Kumosinski, *J. Phys. Chem. B* **1997**, *101*, 2224.
- [4] A. Ray, M. Feng, H. Tachikawa, *Langmuir* **2005**, *21*, 7456.
- [5] H. Y. Lu, J. Yang, J. F. Rusling, N. F. Hu, *Electroanalysis* **2006**, *18*, 379.
- [6] J. Yang, N. F. Hu, *Bioelectrochem. Bioenerg.* **1999**, *48*, 117.
- [7] H. Zhou, Z. Chen, R. W. Yang, L. B. Shang, G. X. Li, *J. Chem. Technol. Biotechnol.* **2006**, *81*, 58.
- [8] J. T. Pang, C. H. Fan, X. J. Liu, T. Chen, G. X. Li, *Biosens. Bioelectron.* **2003**, *19*, 441.
- [9] C. H. Fan, H. Y. Wang, S. Sun, D. X. Zhu, *Anal. Chem.* **2001**, *73*, 2850.
- [10] X. L. Luo, A. J. Killard, M. R. Smyth, *Electroanalysis* **2006**, *18*, 1131.
- [11] R. F. Gao, J. B. Zheng, L. F. Qiao, *Electroanalysis* **2010**, *22*, 1084.
- [12] K. Qiao, H. Y. Liu, N. F. Hu, *Electrochim. Acta* **2008**, *53*, 4654.
- [13] J. X. Wang, M. X. Li, Z. J. Shi, N. Q. Li, Z. N. Gu, *Anal. Chem.* **2002**, *74*, 1993.
- [14] P. L. He, N. F. Hu, J. F. Langmuir **2004**, *20*, 722.
- [15] D. F. Cao, P. L. He, N. F. Hu, *Analyst* **2003**, *128*, 1268.
- [16] H. Zhang, H. Y. Lu, N. F. Hu, *J. Phys. Chem. B* **2006**, *110*, 2171.
- [17] L. Y. Zhao, H. Y. Liu, N. F. Hu, *Anal. Bioanal. Chem.* **2006**, *384*, 414.
- [18] Y. Wang, W. P. Qian, Y. Tan, S. H. Ding, H. Q. Zhang, *Talanta* **2007**, *72*, 1134.
- [19] D. Shan, S. X. Wang, H. G. Xue, S. Cosnier, *Electrochem. Commun.* **2007**, *9*, 529.
- [20] M. C. Buzzeo, C. Hardacre, R. G. Compton, *Anal. Chem.* **2004**, *76*, 4583.
- [21] P. He, H. T. Liu, Z. Y. Li, Y. Liu, X. D. Xu, J. H. Li, *Langmuir* **2004**, *20*, 10260.
- [22] P. Yu, Y. Q. Lin, L. Xiang, L. Su, J. Zhang, L. Q. Mao, *Langmuir* **2005**, *21*, 9000.
- [23] N. Maleki, A. Safavi, F. Tajabadi, *Anal. Chem.* **2006**, *78*, 3820.
- [24] W. Sun, R. F. Gao, K. Jiao, *J. Phys. Chem. B* **2007**, *111*, 4560.
- [25] W. Sun, X. Q. Li, Y. Wang, X. Li, C. Z. Zhao, K. Jiao, *Bioelectrochemistry* **2009**, *75*, 170.
- [26] W. Sun, D. D. Wang, G. C. Li, Z. Q. Zhai, R. J. Zhao, K. Jiao, *Electrochim. Acta* **2008**, *53*, 8217.
- [27] W. Sun, X. Q. Li, P. Qin, K. Jiao, *J. Phys. Chem. C* **2009**, *113*, 11294.
- [28] H. Huang, N. F. Hu, Y. H. Zeng, G. Zhou, *Anal. Biochem.* **2002**, *308*, 141.
- [29] L. V. Bindhu, E. T. J. Abraham, *J. Appl. Polym. Sci.* **2003**, *88*, 1456.
- [30] M. H. Yang, Y. H. Yang, B. Liu, G. L. Shen, R. Q. Yu, *Sens. Actuators B* **2004**, *101*, 269.
- [31] C. Peniche, W. Arguelles-Monal, H. Peniche, *Macromol. Biosci.* **2003**, *3*, 511.
- [32] W. Xiao, J. S. Chen, C. M. Li, R. Xu, X. W. Lou, *Chem. Mater.* **2010**, *22*, 746.
- [33] P. George, C. Hanania, *Biochem. J.* **1953**, *55*, 236.
- [34] W. Sun, D. D. Wang, R. F. Gao, K. Jiao, *Electrochem. Commun.* **2007**, *9*, 1159.
- [35] A. J. Bard, L. R. Faulkner, *Electrochemical Methods*, Wiley, New York **1980**.
- [36] E. Laviron, *J. Electroanal. Chem.* **1974**, *52*, 355.
- [37] E. Laviron, *J. Electroanal. Chem.* **1979**, *101*, 19.
- [38] A. B. Moghaddam, M. R. Ganjali, R. Dinarvand, *Biophys. Chem.* **2008**, *134*, 25.
- [39] C. Y. Liu, J. M. Hu, *Biosens. Bioelectron.* **2009**, *24*, 2149.
- [40] W. Sun, Y. Wang, X. Q. Li, J. Wu, T. R. Zhan, K. Jiao, *Electroanalysis* **2009**, *21*, 2454.
- [41] W. Sun, P. Qin, R. J. Zhao, K. Jiao, *Talanta* **2010**, *80*, 2177.
- [42] R. A. Kamin, G. S. Wilson, *Anal. Chem.* **1980**, *52*, 1198.
- [43] Z. Q. Zhai, J. Wu, W. Sun, K. Jiao, *J. Chin. Chem. Soc.* **2009**, *56*, 561.
- [44] S. F. Wang, T. Chen, Z. L. Zhang, X. C. Shen, Z. X. Lu, D. W. Pang, K. Y. Wong, *Langmuir* **2005**, *21*, 9260.
- [45] A. K. M. Kafi, F. Yin, H. K. Shin, Y. S. Kwon, *Thin Solid Films* **2006**, *499*, 420.
- [46] W. Sun, R. F. Gao, X. Q. Li, D. D. Wang, M. X. Yang, K. Jiao, *Electroanalysis* **2008**, *20*, 1048.
- [47] X. B. Lu, G. F. Zou, J. H. Li, *J. Mater. Chem.* **2007**, *14*, 1427.
- [48] J. J. Feng, G. Zhao, J. J. Xu, H. Y. Chen, *Anal. Biochem.* **2005**, *342*, 280.